

https://doi.org/10.1070/QEL17584

Investigation of the transition at a wavelength of 506 nm, intended for deep cooling of thulium atoms

D.I. Provorchenko, D.O. Tregubov, D.A. Mishin, A.A. Golovizin, E.S. Fedorova, K.Yu. Khabarova, V.N. Sorokin, N.N. Kolachevsky

Abstract. **A scheme is proposed for the third stage of laser cooling of thulium atoms at a wavelength of 506.2 nm, and a system for stabilising the laser radiation frequency is described, which provides the required characteristics. The transition $|4f^{13}(2F^{o})6s^{2}, J = 7/2\rangle \rightarrow |4f^{13}\times (2F^{o}_{7/2})6s6p, J = 9/2\rangle$ at a wavelength of 506.2 nm is detected in a magneto-optical trap with the employment of the developed laser setup. The value of hyperfine splitting of the transition upper level is measured, and the single-dimension cooling at this wavelength is observed for the first time.**

Keywords: *spectroscopy, hyperfine splitting, optical clock, laser cooling, ultracold atoms, thulium.*

1. Introduction

With the appearance of optical clocks, which characteristics surpass those of caesium frequency standards, wide prospects were opened for their employment in practice and fundamental studies. The most accurate optical clocks are used for verifying fundamental theories [1], determining limitations on fundamental constant drifts [2], and dark matter search [3]. Some problems related to investigations of the Earth gravitational field and navigation require transportable systems [4]. Compact mobile optical standards are actively developed in Russia [5, 6], China [7], Europe [8–10], and USA [11]. Most of them are based on single ions, which is explained by the relative simplicity of trapping and cooling of such ions. Transportable clocks on neutral atoms described in [8, 12] demonstrate a better stability than on single ions; however, they have worse mass and dimension characteristics, are more complicated in adjustment and differ by a substantial frequency shift due to a black body radiation.

Black body radiation and radiation of an optical lattice are the main reasons for the shift of the clock transition frequency in optical clocks on neutral atoms [13]. However, it was shown in [14], that the clock transition at a wavelength of 1.14 μm in neutral thulium has a very low sensitivity to black body radiation as compared to transitions in other atoms (3000 times less than in strontium atoms) and certain ions. The employment of thulium in optical clocks solves the problem of the hardly controllable frequency shift related to black body radiation. Nevertheless, the problem remains, which relates to an optical lattice radiation. The use of a magic wavelength for the optical lattice eliminates the intensity-linear frequency shift related to polarisability from dipole electric transitions. Contributions from higher-order polarisabilities and hyperpolarisability remain and may reveal at a relative instability of 10^{-17}–10^{-18}, with the frequency shift values depending on the filling of levels in the potential of the optical lattice, that is, on the atom temperature [15, 16]. A lower temperature substantially simplifies calculations of the contributions from higher-order polarisabilities and experimental control of the latter.

The minimal temperature of thulium atoms obtained in our previous experiments was 10 μK [17]. It was attained by two stages of laser cooling, the final temperature being determined by the second cooling stage with the employment of the transition at a wavelength of 530.7 nm, which has a natural width of 350 kHz (Fig. 1). In experiments on constructing optical clocks, the minimal temperature of an atomic cloud just before trapping into an optical lattice was 10 μK as well [14]. The temperature, at which the population of the ground state prevails in the optical lattice potential, should be less than 2.5 μK for the characteristic optical lattice potential (about $300E_{\rm rec}$, where $E_{\rm rec} = h \times 1$ kHz is the photon recoil energy, and h is the Plank constant), used in our experiment.

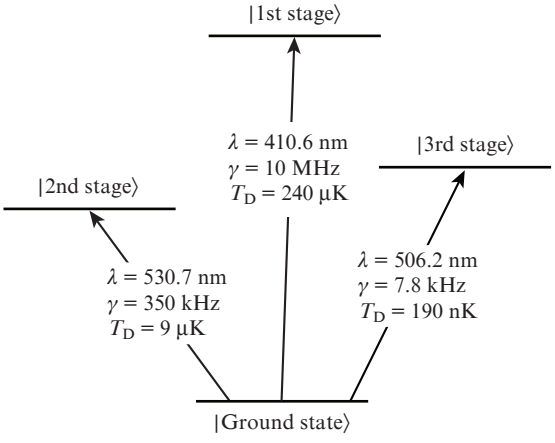

Figure 1. Schematic of three stages for cooling of thulium atoms with indicated values of wavelengths, natural spectral linewidths γ and Doppler temperature limit $T_{\rm D}$ for the employed transitions.

D.I. Provorchenko, D.O. Tregubov, D.A. Mishin, A.A. Golovizin, E.S. Fedorova, V.N. Sorokin Lebedev Physical Institute, Russian Academy of Sciences, Leninskii prosp. 53, 119991 Moscow, Russia; e-mail: provorchenko.di@phystech.edu;
K.Yu. Khabarova, N.N. Kolachevsky Lebedev Physical Institute, Russian Academy of Sciences, Leninskii prosp. 53, 119991 Moscow, Russia; Russian Quantum Centre, Bol'shoi blv. 30, stroenie 1, Skolkovo, 121205 Moscow, Russia

Received 12 March 2021; revision received 12 April 2021
Kvantovaya Elektronika **51** (6) 479–483 (2021)
Translated by N.A. Raspopov

The minimal temperature T attainable under Doppler cooling is related to the width of cooling transition γ by the relationship $T = h\gamma/(2k_B)$. Hence, a deeper cooling requires a transition with a less spectral width. In thulium atom, there is the cyclic transition $|4f^{13}(2F^o)6s^2, J = 7/2\rangle \rightarrow |4f^{13}(2F^o_{7/2})6s6p, J = 9/2\rangle$ at a wavelength of 506.2 nm with a natural linewidth of 7.8 kHz [18]. On this transition, a third cooling stage can be realised. The spectral width of the transition should provide a lower cloud temperature (the Doppler limit is 190 nK) at a sufficiently high cooling rate. A schematic diagram of levels and some characteristics for all the three cooling stages are presented in Fig. 1. The employment of narrow transitions with a natural spectral width of ~1 kHz for deep laser cooling has been successively demonstrated on Sr, Er, and Dy atoms [19–22]. The Doppler temperature level in this case becomes comparable with the limiting recoil energy, and the confining force in a magneto-optical trap (MOT) becomes comparable with the gravitation force. The employment of such transitions makes it possible to reach a thulium atom temperature in MOT below 1 μK [20].

Thulium atom cooling on the suggested transition is a realisable task taking into account a sufficiently low atomic temperature in the secondary MOT (10 μK). A necessary condition for demonstration of cooling on a narrow transition is a narrow-spectrum laser (with the linewidth less than the transition spectral width) and a possibility to exactly control the detuning of laser radiation frequency relative to the atomic resonance. In the present work, we describe an experiment on stabilising the frequency of laser operated at 506.2 nm by using a transfer-cavity. The detection of the corresponding spectral transition in MOT and first experimental confirmation of thulium atom cooling at this wavelength are also discussed.

2. System for stabilising the cooling laser frequency

For realising the laser cooling on the 506.2-nm transition with a natural linewidth of 7.8 kHz it is necessary to have a narrow-band laser emission red-detuned from the atomic resonance. In the third stage of thulium atom cooling, we use a Toptica DL pro laser as a radiation source. According to the technical specification, the initial spectral linewidth of this laser is about 300 kHz with a long-term frequency instability of about 10 MHz h^{-1}; hence, it is necessary to stabilise the laser frequency and make its spectrum narrower. The standard way to solve this problem is to stabilise the laser frequency relative to an external high-Q resonator according to the Pound–Drever–Hall (PDH) method [23]. However, if there is a well-stabilised reference laser available, the problem of stabilising the cooling laser with a different wavelength can be solved by using a so-called transfer-cavity [24–26]. In this approach, the reference laser is employed for stabilising a length of the cavity, which is then used in a standard PDH scheme for another laser so that the stability of the reference laser is transferred to that laser. To this end, mirrors of the resonator should have high reflection coefficients at the operation wavelengths of both the lasers.

For reference, we used the Toptica DL pro frequency-stabilised laser with the wavelength $\lambda_{ref} = 530.7$ nm, which was employed at the second cooling stage. This laser is stabilised by an external high-Q ULE-cavity according to the PDH method. The ULE finesse is $\mathcal{F} = 1.5 \times 10^5$, the resonator body temperature is stabilised at the zero point of ULE glass linear expansion (33 °C). The spectral mode width of this resonator is 13 kHz, the spectral width of stabilised laser emission line being 100 Hz at most [17]. The residual linear frequency drift is sufficiently small (a characteristic value is 10–100 mHz s^{-1}), and presently it is compensated for every several months by tuning the frequency of one of the acousto-optical modulators incorporated into the optical trace. A scheme with instantaneous frequency adjustment can also be realised similarly to the drift compensation in a clock laser [27].

At the given wavelength of the reference laser $\lambda_{ref} = 530.7$ nm, the transmission signal maxima of the transfer-cavity place the constraint on the resonator length: $L = n\lambda_{ref}/2$ or (in the frequency domain) $L = nc/(2\nu_{ref})$ (n is an integer, and c is the speed of light). For stabilising the resonator length, one of the resonator mirrors is placed on a piezoceramic element, to which a feedback signal is applied. In turn, resonator transmission maxima for the emission of the third-stage-cooling laser with $\lambda = 506.2$ nm place the similar constraint, however, on the frequency of this laser: $\nu = mc/(2L)$ (m is an integer). Thus, the system for stabilising the frequency of the laser at 506.2 nm by the transfer-cavity selects the possible laser frequencies, which are multiples of the transfer-cavity free spectral range $\mathrm{FSR} = c/(2L)$, which at a characteristic transfer-cavity length $L \approx 15$ cm corresponds to $\mathrm{FSR} \approx 1$ GHz. For tuning the laser radiation frequency more accurately, one can choose another length $L' = (n + 1)c/(2\nu_{ref})$, and simultaneously change a frequency of the mode used for stabilising the cooling laser: $\nu = (m + 1)c/(2L')$. Thus, the step for choosing the frequency of a 506.2-nm laser becomes substantially smaller:

$$\nu' - \nu = \mathrm{FSR}\frac{m-n}{n+1} \approx \mathrm{FSR}\left(\frac{\nu}{\nu_{ref}} - 1\right) \approx 45\ \mathrm{MHz}. \qquad (1)$$

By varying the temperature of the resonator, the resonator length is chosen in such a way that the required resonator mode would fit the centre of the tuning range controlled by the piezoceramic element. In case of an accidental failure in the feedback loop, the system will lock again to the same mode. For a frequency shift of 45 MHz, the resonator temperature should be changed by approximately 0.1 °C. The final adjustment of the laser emission frequency to the atomic transition frequency is performed by using an acousto-optical modulator (AOM) (Fig. 2).

The transfer-cavity is formed by two mirrors separated by a distance of 15 cm (FSR = 1 GHz). A plane input mirror is mounted on the cylindrical piezoceramic actuator which controls the resonator length. The output spherical mirror has a radius of curvature $R = 204$ mm. A resonator spatial mode is matched to an input radiation by using a lens with a focal length $f_L = 50$ cm. At wavelengths of 530.7 and 506.2 nm, the transmission of input mirror is 0.36% and 3.9%, respectively, and output mirror transmission is 0.067% and 0.1%, respectively. A calculated transfer-cavity finesse should be: $\mathcal{F}_1 = 1500$ at the wavelength of 530.7 nm and $\mathcal{F}_2 = 135$ at 506.2 nm. Nevertheless, the actual values are substantially less: $\mathcal{F}_1 = 223$ and $\mathcal{F}_2 = 40$, which indicates that optical losses on resonator mirrors are sufficiently high. In future, we are going to change the mirrors in order

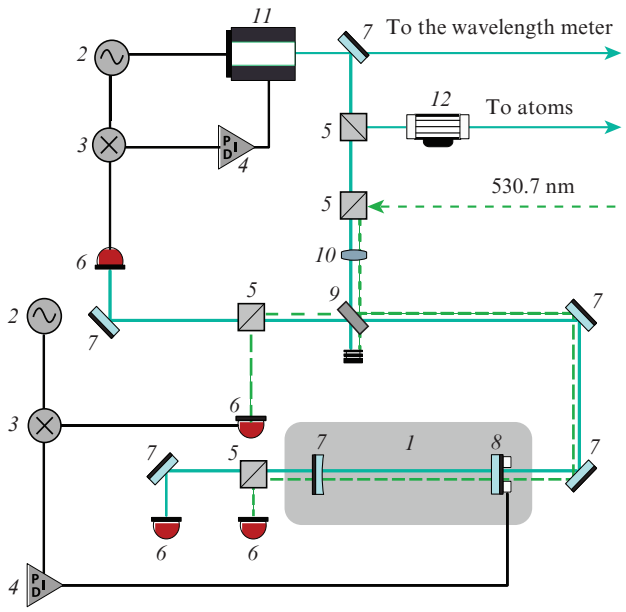

Figure 2. Optical scheme for stabilising the length of the transfer-cavity with simultaneous stabilisation of laser radiation frequency at 506.2 nm to an eigenmode of the transfer-cavity:
(*1*) transfer-cavity; (*2*) RF oscillator; (*3*) RF mixer; (*4*) PID-controller; (*5*) polarisation beam splitter; (*6*) photodiode; (*7*) dielectric mirror; (*8*) mirror on a piezoceramic actuator; (*9*) 50/50 splitter; (*10*) matching lens; (*11*) laser at 506.2 nm; (*12*) AOM.

to obtain $\mathcal{F} \sim 1000$ at both wavelengths. It will improve the stabilisation quality by one order and more. In this case, the width of the resonator mode will be ~1 MHz, and the expected linewidth of stabilised laser emission is less by several orders in magnitude.

The radiation reflected from the resonator is detected by a fast photodetector for stabilising the resonator length by the PDH method. To this end, a photodiode signal is mixed in a phase detector ZRPD (Mini Circuits) with the reference signal at the frequency of reference laser current modulation $f =$ 10.7 MHz (a relative phase between the two signals is corrected by choosing an appropriate cable length or varying slightly the frequency of the modulation signal). The error signal formed by the phase detector, passed to the PID-controlled, which was realised as a single-board computer Red Pitaya with FPGA [28]. The feedback signal is applied to the piezoceramic, which stabilises the resonator length.

For stabilising the radiation frequency of the laser operated at 506.2 nm, a signal from the photodiode passes to a laser control unit, where it is converted to the error signal by an internal PDH-unit (the frequency of laser diode current modulation is $f = 25$ MHz). The PID-controller is realised in the second channel of the same single-board computer Red Pitaya.

The quality of resonator stabilisation by the reference laser ($\lambda = 530.7$ nm) and of the 506.2 nm laser by the resonator mode is analysed by using the transmission signal of the transfer-cavity; typical transmission is presented in Fig. 3. A noise level of the transmission signal is determined by power fluctuations of the radiation passed through a fibre and by its polarisation fluctuations. It is possible to maintain stabilisation of the laser radiation to a certain mode of the transfer-cavity for several hours.

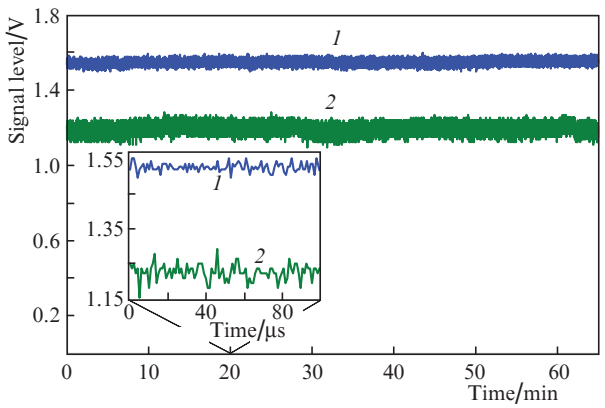

Figure 3. Voltage signals of photodiodes detecting the transfer-cavity transmission for the laser radiation at (*1*) 506.2 and (*2*) 530.7 nm. Signal noise at short time intervals (in the insertion) is explained by a high amplification and high-frequency noises of the photodiode.

3. Experiment

For performing an experiment on detection of the transition at 506.2 nm in thulium atoms and for verifying possibilities of the laser cooling, a laser system was assembled, which produced a single-dimension molasses at this wavelength and crossed the MOT domain. A linearly polarised laser radiation passed to a vacuum chamber in the horisontal plane and reflected backward. It was possible to screen the reflected radiation for exciting atoms by a single beam. An additional radiation at a wavelength of 418.8 nm, which is used for optical pumping [29] was introduced into the fibre for adjusting optical elements and matching molasses with MOT. A CMOS camera placed above detects the spatial distribution and number of atoms by the luminescence signal at the wavelength of 410.6 nm in a probe beam of the resonance radiation, which is also used at the first cooling stage.

3.1. Hyperfine splitting

The nuclear spin of the only stable thulium isotope is $I = 1/2$; hence, each electron level splits into two hyperfine components. The laser cooling occurs on the transition between lower hyperfine components of levels ($F = 4 \rightarrow F' = 5$). The desired transition was found from spectroscopy of transitions in MOT during the second stage of laser cooling (see Table 1). Similarly to experiments in [29], transitions from the lower (by energy) hyperfine component of the ground state ($F = 4$) are detected by a reduction of the number of atoms in MOT. Transitions from the upper component ($F = 3$) are detected by an increase in the number of atoms, because in this case the laser at 506.2 nm plays the role of a repumping laser and returns atoms to the initial cooling cycle.

Table 1. Frequencies of transitions between the hyperfine components of levels for the third cooling stage.

Transition between hyperfine components	Frequency/GHz
$F = 4 \rightarrow F' = 5$	592045.689
$F = 4 \rightarrow F' = 4$	592049.163
$F = 3 \rightarrow F' = 4$	592047.666
$F = 3 \rightarrow F' = 5$	Forbidden

In this experiment, the laser at 506.2 nm has not been stabilised by the transfer-cavity. The measurement accuracy for all frequencies is determined by the inaccuracy of a wavelength-measuring instrument and equals 0.1 GHz, and the accuracy of a frequency difference is determined by a short-term stability of this instrument and equals 7 MHz [30]. From the measurements taken, we have found values of hyperfine splitting for both levels of the transition. For the ground level, the value obtained 1497(7) MHz agrees with previously known value of 1496.550(1) MHz [31]. For the upper level $|4f^{13}(2F^{o}_{7/2})6s6p, J = 9/2\rangle$, the value obtained is 3474(7) MHz, which well coincides with the result 3474(2) MHz measured in [32]. The level $F = 5$ is below in energy than the level $F = 4$.

The transition that was used for laser cooling ($F = 4 \rightarrow F' = 5$) has been studied in more details. To this end, the radiation frequency of the laser operated at 506.2 nm was stabilised by the transfer-cavity to the frequency of 592045.498 GHz according to results of wavelength measurements. Scanning the AOM frequency over the resonance transition made it possible to find more exactly the line central position and its spectral width that was 560(30) kHz (Fig. 4).

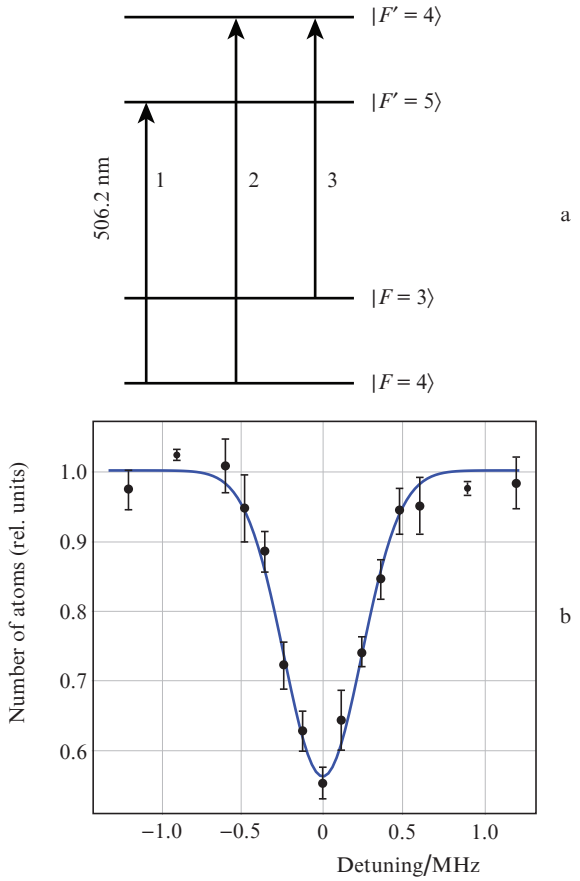

Figure 4. Hyperfine components of the transition at the wavelength of 506.2 nm in thulium atom (transitions 1 and 2 were determined from a reduction of the number of atoms in MOT, transition 3 was found from an increase in this number) (a), and the reduction of the number of atoms in MOT while scanning the AOM frequency over the resonance transition 1 ($F = 4 \rightarrow F' = 5$) (b). Solid curve is a Gaussian profile approximation.

The linewidth measured is substantially greater than the natural width, which is inherent in MOT spectroscopy. In details, the Doppler broadening at the atomic temperature of 20 μK is about 150 kHz. The difference in g-factors for the ground and upper levels (1.14 and 1.29, respectively [18]) results in the broadening related to the magnetic field in trap and is about 300 kHz. The broadening due to the laser radiation in the experimental conditions is about 150 kHz (at the radiation power of 100 μW and beam diameter of 0.7 mm). The transition linewidth observed can be reduced by exactly defining a quantisation axis, using optical pumping, and reducing a power of the probe radiation. Note that our aim in this case was, mainly, search for and identification of the transitions.

3.2. Single-dimension optical molasses

In the first tests, which might testify the efficiency of the third cooling stage, we verified an influence of a single-dimension molasses on the size of the atomic cloud in the direction of the cooling beams. After finishing the second stage of MOT, the optical field of the second cooling stage switched off, and the magnetic field gradient was reduced to 1/5 of the initial value (similarly to experiments with deep cooling of strontium atoms [19, 20]). Then the optical molasses at the wavelength of 506.2 nm switched on for a time $\tau \approx 7$ ms, and then the radius of the atomic cloud was measured (at the 1/e level) along the optical molasses axis. A pulsed scheme of the experiment is given in the insertion of Fig. 5. The laser radiation frequency was scanned by using an AOM, whereas the laser at 506.2 nm was stabilised by the transfer-cavity.

The dependence of the atomic cloud radius on frequency detuning (circles in Fig. 5) demonstrates the effect of reduced cloud dimension under detuning to the red spectral range from the resonance centre. This was confirmed in another experiment with more thorough scanning of the AOM frequency (points in Fig. 5). This peculiarity in the spectrum with a width of about 200 kHz testifies that the spectral line-

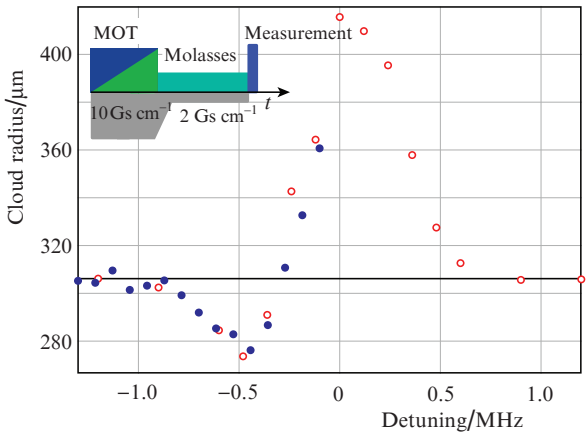

Figure 5. Size of atomic cloud along the optical molasses Vs. the detuning of the radiation frequency from resonance (circles) and the same dependence in more details observed in other experiment (points). Solid curve is the cloud size with lacking radiation at 506.2 nm. In the insertion: a sequence of switching on laser pulses and magnetic fields in the experiment.

width of the stabilised laser is less than this value. The coincidence of spectra taken with an accuracy better than 50 kHz at different times testifies that the laser frequency instability is bounded above at times of about an hour. In addition, a reduction of the atomic cloud size means that the velocity of the atom escape falls, that is, the atomic temperature reduces and/or a confining force is present.

4. Conclusions

The transfer-cavity is developed and studied, which was used for stabilising a laser with the wavelength of 506.2 nm intended for the third stage of thulium atom cooling. Although the finesse of the transfer-cavity (40 – 150 depending on the wavelength) is not high, the designed system made it possible to realise spectroscopy of the thulium transition $|4f^{13}(2F^{o})6s^{2}, J = 7/2\rangle \rightarrow |4f^{13}(2F^{o}_{7/2})6s6p, J = 9/2\rangle$ at a wavelength of 506.2 nm. All the three hyperfine components of the transition at 506.2 nm was detected in the secondary MOT, and the value of hyperfine splitting of the upper transition level was measured 3474(7) MHz. For the transition component intended for laser cooling, the absorption spectrum and dependence of atomic cloud dimension on the radiation frequency detuning from resonance were measured. A reduction of atomic cloud dimension under the action of the radiation at 506.2 nm was observed in a relatively narrow spectral range of 200 kHz with the laser frequency stabilised by the transfer-cavity. This confirms the reduction of the atomic temperature along the axis of optical molasses.

Results obtained testify that the frequency stabilisation of the laser at 506.2 nm is better than 50 kHz at time intervals of about an hour. In the near future, we plan to change mirrors of the transfer-cavity for increasing its finesse, which will make the laser linewidth substantially narrower and improve its stability to required values of about 1 kHz. After that, an experimental MOT at this wavelength will be tested.

Acknowledgements. The work was supported by the Russian Science Foundation (Grant No. 19-72-00174).

References

1. Sanner C., Huntemann N., Lange R., Tamm C., Peik E., Safronova M.S., Porsev S.G. *Nature*, **567**, 204 (2019).
2. Safronova M.S., Porsev S.G., Sanner C., Ye J. *Phys. Rev. Lett*., **120**, 173001 (2018).
3. Derevianko A., Pospelov M. *Nature Phys*., **10**, 933 (2014).
4. Delehaye M., Lacroûte C. *J. Mod. Opt*., **65**, 622 (2018).
5. Semerikov I.A., Khabarova K.Yu., Zalivako I.V., Borisenko A.S., Kolachevsky N.N. *Bull. Lebedev Phys. Inst*., **45**, 337 (2018) [*Kratk. Soobshch. Fiz. FIAN*, (11), 14 (2018)].
6. Chepurov S.V., Lugovoy A.A., Prudnikov O.N., Taichenachev A.V., Bagaev S.N. *Quantum Electron*., **49**, 412 (2019) [*Kvantovaya Electron*., **49**, 412 (2019)].
7. Cao J., Zhang P., Shang J., Cui K., Yuan J., Chao S., Wang S., Shu H., Huang X. *Appl. Phys. B: Lasers Opt*., **123**, 112 (2017).
8. Grotti J., Koller S., Vogt S., Häfner S., et al. *Nature Phys*., **14**, 437 (2018).
9. Hannig S., Pelzer L., Scharnhorst N., Kramer J., et al. *Rev. Sci. Instrum*., **90**, 53204 (2019).
10. Ritter S., Hafiz M.A., Arar B., Bawamia A., et al. *Proc. OSA Quantum 2.0 Conf*. (OSA, 2020) paper QTh5B.6; https://doi.org./10.1364/QUANTUM.2020.QTh5B.6.
11. Brewer S.M., Chen J.S., Leibrandt D.R., Chou C.W., Wineland D.J., Bergquist J.C., Rosenband T. *Proc. 2014 IEEE Int. Frequency Control Symp*. (IFCS) (Taipei, Taiwan, 2014) p.1. DOI:10.1109/FCS.2014.6859999.
12. Takamoto M., Ushijima I., Ohmae N., Yahagi T., Kokado K., Shinkai H., Katori H. *Nature Photon*., **14**, 411 (2020).
13. Ludlow A.D., Boyd M.M., Ye J., Peik E., Schmidt P.O. R*ev. Mod. Phys*., **87**, 637 (2015).
14. Golovizin A., Fedorova E., Tregubov D., Sukachev D., Khabarova K., Sorokin V., Kolachevsky N. *Nat. Commun*., **10**, 1 (2018).
15. Brown R.C., Phillips N.B., Beloy K., McGrew W.F., et al. *Phys. Rev. Lett*., **119**, 253001 (2017).
16. Ushijima I., Takamoto M., Katori H. *Phys. Rev. Lett*., **121**, 263202 (2018).
17. Vishnyakova G.A., Golovizin A.A., Kalganova E.S., Sorokin V.N., Sukachev D.D., Tregubov D.O., Khabarova K.Yu., Kolachevsky N.N. *Phys. Usp*., **59**, 168 (2016) [*Usp. Fiz. Nauk*, **186** (2), 176 (2016)].
18. Kramida A., Ralchenko Yu., Reader J. NIST ASD Team. NIST Atomic Spectra Database (ver. 5.8) (2021); https://doi.org/10.18434/T4W30F.
19. Loftus T.H., Ido T., Ludlow A.D., Boyd M.M., Ye J. *Phys. Rev. Lett*., **93**, 073003 (2004).
20. Loftus T.H., Ido T., Boyd M.M., Ludlow A.D., Ye J. *Phys. Rev. A: At. Mol. Opt. Phys*., **70**, 063413 (2004).
21. Berglund A.J., Hanssen J.L., McClelland J.J. *Phys. Rev. Lett*., **100** (11), 113002 (2008).
22. Lu M., Burdick N.Q., Youn S.-H., Lev B.L. *Phys. Rev. Lett*., **107**, 190401 (2011).
23. Drever R.W.P., Hall J.L., Kowalski F.V., et al., *Appl. Phys. B: Photophys. Laser Chem*., **31**, 97 (1983).
24. Bohlouli-Zanjani P., Afrousheh K., Martin J.D.D. *Rev. Sci. Instrum*., **77**, 093105 (2006).
25. Zhao W.Z., Simsarian J.E., Orozco L.A., Sprouse G.D. *Rev. Sci. Instrum*., **69**, 3737 (1998).
26. Riedle E., Ashworth S.H., Farrell J.T., Nesbitt D.J. *Rev. Sci. Instrum*., **65**, 42 (1994).
27. Golovizin A., Bushmakin V., Fedorov S., Fedorova E., et. al. *J. Russ. Laser Res*., **40**, 540 (2019).
28. https://www.redpitaya.com/ (2021).
29. Fedorova E., Golovizin A., Tregubov D., Mishin D., et al. *Phys. Rev. A*, **102**, 63114 (2020).
30. Tregubov D.O., Golovizin A.A., Fedorova E.S., et al. *Quantum Electron*., **50**, 566 (2020) [*Kvantovaya Electron*., **50**, 566 (2020)].
31. Ritter G.J. *Phys. Rev*., **128**, 2238 (1962).
32. Kröger S., Tanriver L., Kronfeldt H.D., Guthöhrlein G., Behrens H.O. *Z. Phys. D*, **41**, 181 (1997).